Hindawi
International Journal of Photoenergy
Volume 2019, Article ID 5092078, 12 pages
https://doi.org/10.1155/2019/5092078

Research Article

Sliding Mode Controllers for Standalone PV Systems: Modeling and Approach of Control

Y. Chaibi,[1] **M. Salhi**,[1] **and A. El-jouni**[2]

[1]*2EMI Team, ENSAM, Moulay Ismail University, B.P 15290 El Mansour Meknes, Morocco*
[2]*Physics Department, "Centre Régional des Métiers d'Education et de Formation" (CRMEF), Tangier, Morocco*

Correspondence should be addressed to Y. Chaibi; chaibi.yassine@gmail.com

Received 26 July 2018; Revised 20 November 2018; Accepted 2 December 2018; Published 5 March 2019

Academic Editor: Mahmoud M. El-Nahass

This paper presents a single-phase standalone photovoltaic (PV) system with two stages of converters. The aim of this work is to track the maximum power point (MPP) so as to transfer the maximum available power to the load and to control the output current in order to feed the AC load by a sinusoidal current. These goals are attained by using the sliding mode to design control laws in order to command the boost DC-DC and the inverter switches. Thus, a maximum power point tracking (MPPT) and an output current controller based on the sliding mode are proposed. The innovative aspect of this work is to propose a standalone PV system with the controllers based only on the sliding mode control approach. The proposed system is modeled and simulated under MATLAB Simulink under fast variations of irradiance and temperature. Then, the obtained results using the suggested MPPT are compared to those using the incremental conductance (IC) method. These results demonstrate the superiority of the sliding mode MPPT in terms of the tracking speed, the efficiency, and the time of response. Moreover, the current controller provides an output current of high quality with a THD of 3.47%. Furthermore, for accurate results, these controllers are evaluated under the fluctuations of two daily climatic profiles (sunny and cloudy) and compared those of the IC method. The results illustrate that the sliding mode MPPT has the potential of generating more electrical energy than the IC MPPT with benefits of up to 13.02% for the sunny daily profile and 27.57% for the cloudy one.

1. Introduction

Due to the increasing fuel prices and related environmental concerns, renewable energies become an important source to supply electricity to buildings and industrial sectors. Power generation from these sources possesses many outcomes such as clean and limitless behavior [1, 2]. Wind, hydro, geothermal, and solar energies have been available since the birth of our planet and have been used by the first human generation in different ways. Nowadays, the exploitation of these energies knows a remarkable improvement taking profit from the accelerated technological advances [3]. Solar energy is considered among the fast-developing technologies and experiences a considerable drop in equipment costs. More specifically, solar photovoltaic (PV) systems are becoming cost-effective options and have the capability of competing with conventional power generation processes [2, 4]. However, the drawbacks of these systems are the low efficiency of the PV module (9 to 16%) and the nonlinear behavior of the PV cell power-voltage (P-V) characteristic [5].

In order to overcome these complications, many solutions are proposed to improve the performance of the PV systems. As the most important solution, maximum power point tracking techniques represent a key solution to reach the optimal point of the PV module and stay at this point. In the literature, several works reported the use of various MPPT methods in different PV applications [6, 7]. Perturb and Observe (P&O) technique is widely used to extract the MPP. This technique is based on the fact of perturbing the input voltage or current and observing the response of the system until reaching the optimal point. Furthermore, The P&O technique is known by its simple algorithm which facilitates the implementation. However, its performances are discussed especially the oscillation around the MPP [8, 9]. To reduce the latter, the incremental conductance (IC)

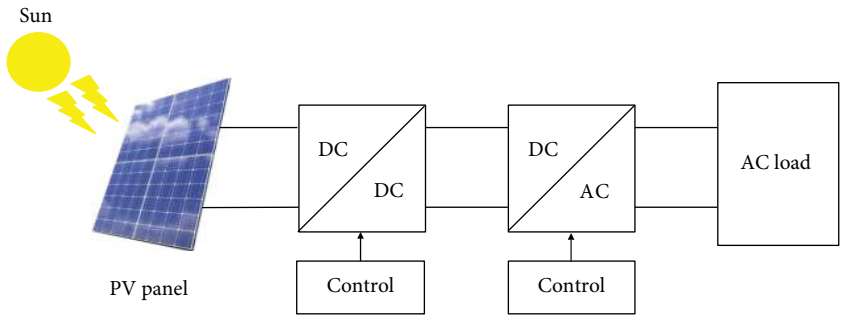

Figure 1: Standalone PV system.

method has been proposed. The latter has corrected partially the oscillation problem. Since this technique is based on the instant comparison of the conductance I/V with the increment of the conductance $\Delta I/\Delta V$, the maximum power point is reached only if both quantities are equal [10, 11]. Thus, for low irradiance variations, it is hard to determine the exact location of this MPP which causes some power losses and reduces the overall efficiency of the PV system. To overcome these complications, other improved MPPT algorithms have been proposed, based on artificial intelligence [12, 13] or genetic algorithms [14]. These techniques proved high superiority in terms of tracking the MPP since they reach the maximum power immediately regardless of any sudden change of the atmospheric conditions and without oscillation in the steady state [15]. But most of these techniques require calculators of high performance which makes them costly and complex to implement.

In order to find a good compromise between efficiency and simplicity, nonlinear controllers such as back-stepping and sliding mode (SM) have shown various advantages [16, 17]. The implementation simplicity and the robust behavior against the external disturbances encourage the researchers to use these controllers in various PV system applications.

Thanks to its advantages, the sliding mode has been used widely to control variable structure systems (VSS) [17–20]. Accordingly, the switched-mode converters used in PV system applications are the ideal target of this kind of controller [16, 21]. Either it being a DC-DC converter or it being an inverter, the sliding mode control (SMC) has been used widely in the literature.

Kim et al. applied the SM to control the inverter switches in order to force the followed current in the grid to pursue a generated reference current; the simulation and experimental results of this single-stage grid-connected PV system shown that the proposed controller can reduce current overshot and contribute to the optimal design of power devices [22, 23]. Furthermore, Chen et al. proposed to control a DC-DC boost converter feeding a resistive load using a sliding mode in finite time; the obtained results showed good performances in terms of stability and fast response. However, the exploitation of this PV system is focalized only for DC loads. For this reason, Laura et al. used an adaptive SM to manage the control of two stages of converters for a grid-connected PV system. Thus, the controlled converters exhibit robustness properties with a fast response to any sudden irradiance change.

Due to the reported benefits of the sliding mode controllers in terms of robustness and fast response, most researchers used these controllers in grid-connected PV systems [23, 24]. However, the number of works about standalone PV systems is still neglected. For this reason, the purpose of this work is to contribute to the modeling and the simulation of the standalone PV system in Figure 1 and to control both converters using a sliding mode approach. These controllers are described in two parts as follows:

(i) A sliding mode maximum power point tracking (SM-MPPT) of the PV panel with the objective to command the duty cycle of the boost DC-DC in order to extract the MPP rapidly

(ii) Design of a control law by acting on the PWM of the inverter: this control law has a function to force the output current, which circulates in the load to pursue the calculated reference current

To design the proposed controllers, climate changes are considered as perturbations, which affect the overall efficiency of the PV system. Therefore, the proposed system is simulated under a fast variation of solar irradiation and temperature to verify the performance and the stability. Then, in order to validate the simulation results, a comparison with one of the most used method in the literature (incremental conductance) and an estimation of a daily energy is achieved.

This paper is structured as follows: in Section 2, a description of the PV cell and a modeling of the proposed PV system are given. Sections 3 and 4 are dedicated to the MPPT and the current controller, respectively, based on a sliding mode. The effectiveness of these controllers is simulated and discussed in Section 5. Finally, some brief concluding remarks are given in Section 6.

2. Mathematical Modeling of the Standalone PV System

2.1. PV Cell Characteristics. The photovoltaic panel is mostly composed of a set of cells connected in series. This cell can be represented by a p-n junction, which generates electricity when exposed to incident light. In order to analyze the electrical behavior of the PV cell, various equivalent circuit models are reported in the literature [25, 26]. Figure 2 represents one of the most used configurations for PV cell

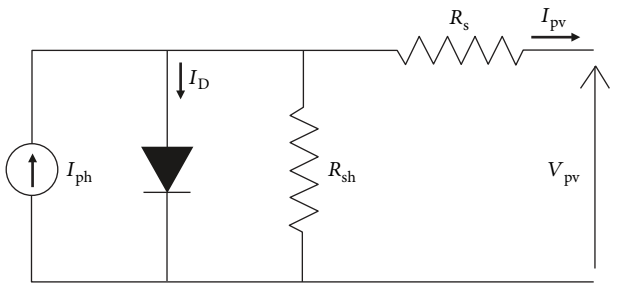

Figure 2: The single-diode model of a PV cell.

modeling by reason of its good performance in the presence of high changes of irradiance and temperature [26].

The electrical equivalent circuit in Figure 2 is composed of a photocurrent generator source I_{ph} in parallel with a diode, the series resistance R_s, and the shunt resistance R_{sh}. By applying Kirchhoff's laws, the output current I_{pv} is expressed by the following equation:

$$I_{pv} = I_{ph} - I_{os}\left\{\exp\left[A\left(V_{pv} + I_{pv}R_s\right) - 1\right]\right\} - \frac{V_{pv} + R_s I_{pv}}{R_{sh}}, \tag{1}$$

where $A = q/\gamma kTN_{cell}$.

The light-generated current I_{ph} variations depend on the measured and the reference values of irradiance and temperature as follows:

$$I_{ph} = \left[I_{sc} + K_i(T - T_{ref})\frac{\lambda}{\lambda_{ref}}\right]. \tag{2}$$

As seen in equation (1), the current that circulates in the diode I_D is expressed by the Shockley equation [27], where I_{os} represents the saturation current and is expressed by the following equation:

$$I_{os} = I_{or}\left(\frac{T}{T_{ref}}\right)^3 \exp\left(\frac{qE_G}{k\gamma}\left[\frac{1}{T} - \frac{1}{T_{ref}}\right]\right). \tag{3}$$

For different applications of the PV energy system, the use of parallel and series panels is depending on the power's need and the used voltage. The main objective of the mathematical modeling of the PV cell is to get an accurate result of the output current and voltage in order to plot the I-V and the P-V characteristics. The latter are plotted in Figure 3. Clearly, the irradiance and the temperature act on the current and the voltage, respectively. Furthermore, the maximum power varies along different irradiance and temperatures.

2.2. Modeling of the PV System. The proposed system in Figure 1 presents a single-phase standalone PV system with an alternative output load. The constitution of this system consists of two stages of static converters with the main objective of ensuring the conversion of the DC energy coming from the PV panel into an AC utility. To begin this study, we must first perform the mathematical modeling by applying the Kirchhoff laws on the detailed system in Figure 4; we found that the system can be written in a set of equations depending on the state of the switches.

The mathematical modeling of the proposed system in a state space leads us to a set of nonlinear equations expressed by the average model as follows:

$$\begin{aligned}
C\frac{\partial v_{pv}}{\partial t} &= i_{pv} - i_1,\\
L\frac{\partial i_L}{\partial t} &= v_{pv} - v_{DC}(1 - \alpha_1),\\
C_{DC}\frac{\partial v_{DC}}{\partial t} &= i_L(1 - \alpha_1) + i_o(1 - 2\alpha_2),\\
L_o\frac{\partial i_o}{\partial t} &= -i_o(R_o + R_c) - v_{DC}(1 - 2\alpha_2),
\end{aligned} \tag{4}$$

where α_1 and α_2 represent the control inputs of the boost converter and the inverter switches, respectively.

The precedent equations can be rewritten in the form $\dot{x} = f(x) + \alpha_1 g_1(x) + \alpha_2 g_2(x)$ where the vectors $\dot{x}, f, g_1$, and g_2 are given as follows:

$$\begin{aligned}
\dot{x} &= \begin{bmatrix} \dot{v}_{pv} \\ i_L \\ \dot{v}_{DC} \\ i_o \end{bmatrix},\\
f(x) &= \begin{bmatrix} \dfrac{i_{pv} - i_l}{C} \\ \dfrac{v_{pv} - v_{DC}}{L} \\ \dfrac{i_L + i_o}{C_{DC}} \\ \dfrac{-i_o(R_o + R_c) - v_{DC}}{L_o} \end{bmatrix},\\
g_1(x) &= \begin{bmatrix} 0 \\ \dfrac{v_{DC}}{L} \\ \dfrac{-i_L}{C_{DC}} \\ 0 \end{bmatrix},\\
g_2(x) &= \begin{bmatrix} 0 \\ 0 \\ \dfrac{-2i_O}{C_{DC}} \\ \dfrac{2v_{DC}}{L_o} \end{bmatrix}.
\end{aligned} \tag{5}$$

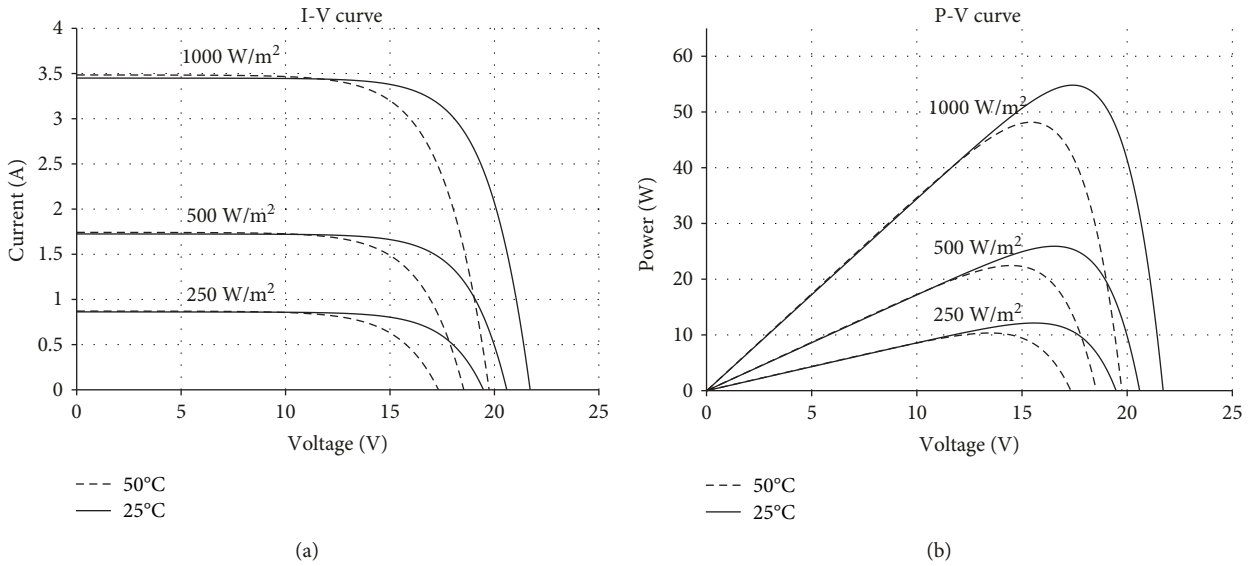

Figure 3: I-V (a) and P-V (b) characteristics of the Mono-Si PV panel SM55 for different levels of irradiance and temperature.

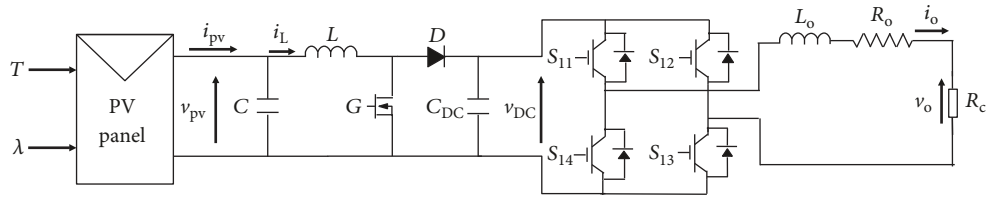

Figure 4: Detailed standalone PV system.

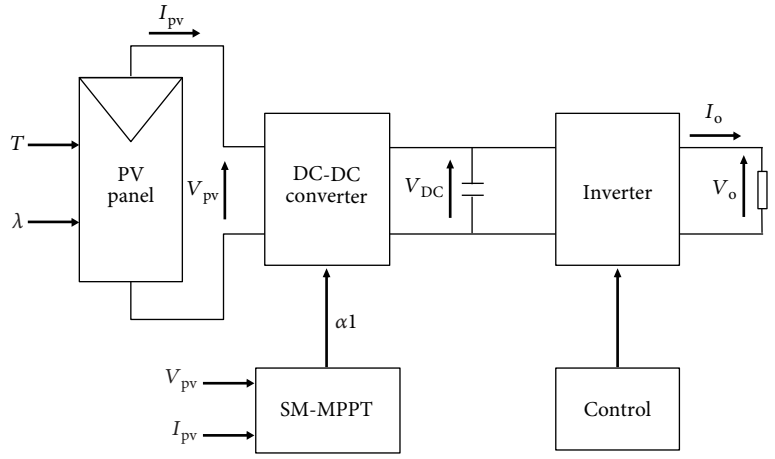

Figure 5: SM-MPPT bloc diagram.

The parametric variations and nonlinearity of PV systems caused by external perturbations as the variation of climate conditions push us to use a robust method with a low sensibility to modeling errors. The sliding mode is a new technique which is characterized by its robustness and admits a convergence in a finite time [28].

The main objective of the sliding mode approach consists to move the trajectory of the variable state of the system to the sliding surface and force this variable to stay in the proximity of this surface. To ensure these conditions, we must design a control law which is adaptive to the variable structure [28].

The main purpose of this paper is to use the sliding mode theory to elaborate a control law which allows us to command both the DC-DC and the DC-AC converters.

3. A Sliding Mode MPPT

The tacking of the maximum power point is the most important operation in photovoltaic systems. In order to

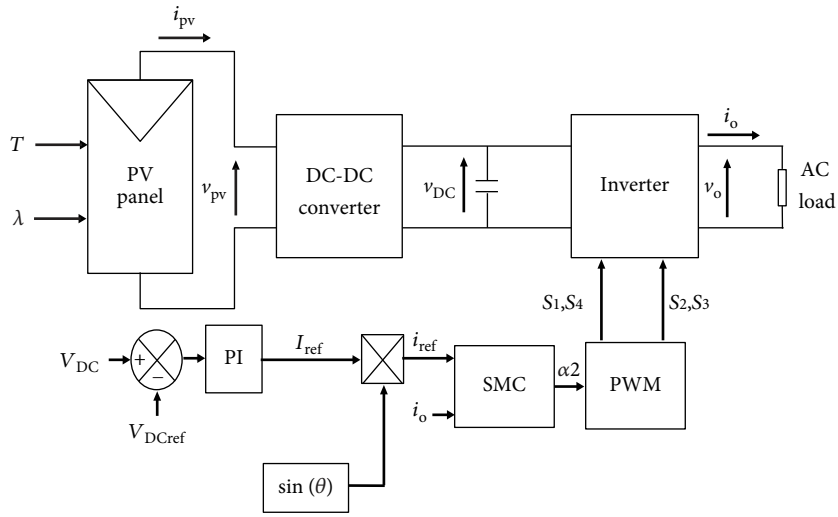

Figure 6: Control strategy followed to elaborate the sliding mode output current controller.

perform the P-V characteristic of the PV panel at its MPP, the derivative of the power with respect to the voltage, i.e., $\partial P_{pv}/\partial V_{pv}$, must converge to zero [29]. For this reason, the sliding mode theory is used to design a control law that acts directly on the duty cycle α_1 of the DC-DC converter as shown in Figure 5.

As the first step of this control law design, the choice of the sliding surface. This surface is a combination of state variables and their references.

In the case of the PV power maximizing, this surface is selected as follows:

$$\sigma_1 = \dot{e}_1 + \gamma_1 e_1, \tag{6}$$

where e_1 is the dynamic error between the regulated output and its reference value which is zero, $e_1 = y_1 = \partial P_{pv}/\partial V_{pv}$, and γ_1 is a positive parameter calculated from the Hurwitz polynomial. The time derivative of this surface is given by

$$\dot{\sigma}_1 = \ddot{e}_1 + \gamma_1 \dot{e}_1. \tag{7}$$

The robust and the stable behavior presents the main advantages of this method [30]; this stability is relative to the attractiveness of this surface and proved by the Lyapunov function presented as follows:

$$V_1 = \frac{1}{2}\sigma_1. \tag{8}$$

In order to provide the asymptotic stability around the equilibrium point, the time derivative of equation (8) must be strictly less than zero ($\dot{V}_1 < 0$); this later can be presented as

$$\dot{V}_1 = \dot{\sigma}_1 \sigma_1. \tag{9}$$

Table 1: Specifications of the Mono-Si PV panel SM55 at the STC.

Parameters	Values
N_{cell}	*36*
P_{MPP} (W)	*55*
V_{MPP} (V)	*17.4*
I_{MPP} (A)	*3.15*
V_{oc} (V)	*21.7*
I_{sc} (A)	*3.45*
K_i (A/K)	*0.0004*

Table 2: PV system parameters used in the simulation.

Parameters	Values
DC-DC boost parameters:	
L (mH)	3.5
C (uF)	4700
C_{DC} (uF)	670
L_o (mH)	2.2
R_o (Ω)	0.7
Sliding mode parameters:	
λ_1	*5000*
λ_2	500
γ_1	150
PI controller coefficients:	
K_p	0.85
K_i	0.001
f (Hz)	50
ω (rad/s)	314.1593

Assuming that the dynamic of the function can be written as $\dot{\sigma}_1 = -\lambda_1 \text{ sign } (\sigma_1)$, equation (9) can be rewritten as

$$\dot{V}_1 = -\lambda_1 |\sigma_1|. \tag{10}$$

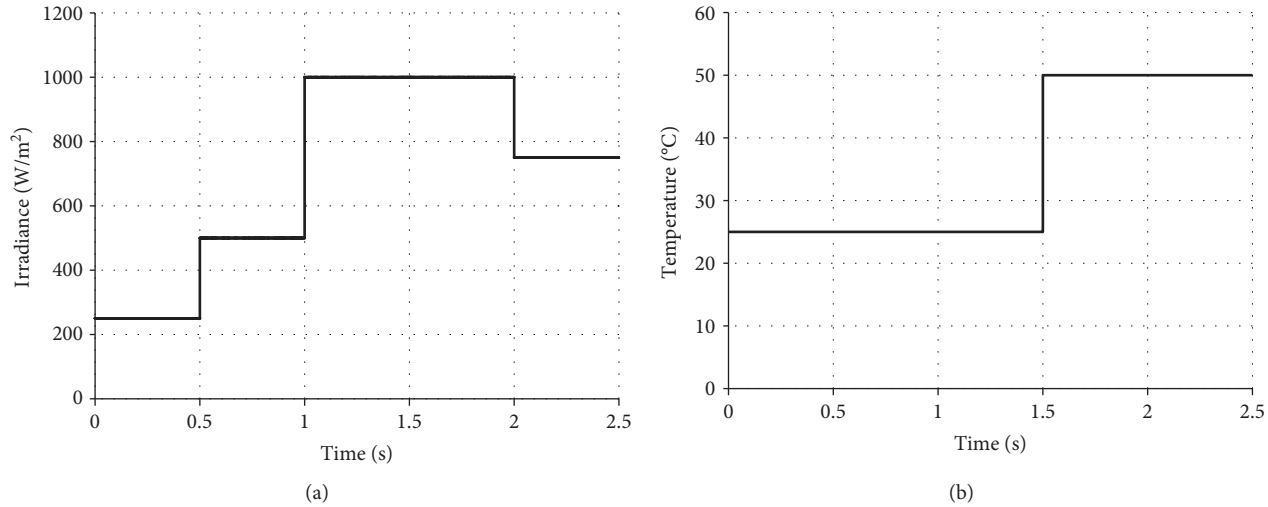

Figure 7: Irradiance (a) and temperature (b) fluctuations used in the simulation.

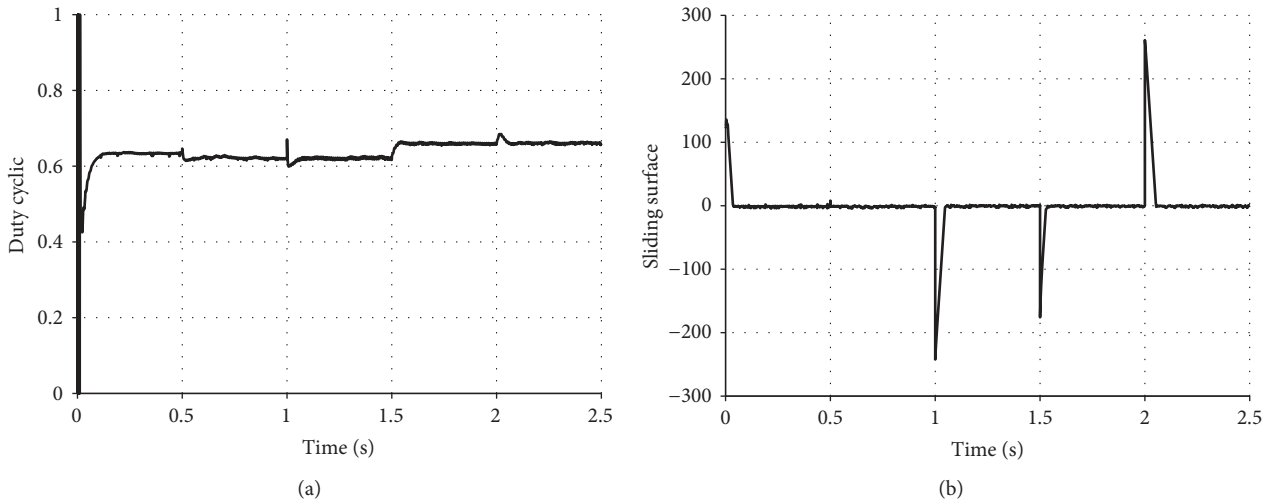

Figure 8: Duty cycle and the sliding surface used to design the control law of the boost converter.

From equation (10) and in order to respect the Lyapunov stability condition, λ_1 must be a positive quantity.

The control law depends totally on the variation of the measured I_{pv} and V_{pv}, and these later vary according to the temperature and the irradiance changes; the strong aspect of the sliding mode MPPT is the stable behavior even with external and parametric variations. In the literature, most MPPT based on a sliding mode used the reduced equation of I_{pv} in order to simplify the calculation; the strong aspect of this study is the use of the detailed calculation to make the results more accurate. As seen in Appendix, all detailed derivatives are demonstrated to design the exact control law.

By replacing (A.3) and (A.4) in equation (7) and using $\dot{\sigma}_1 = -\lambda_1 \text{ sign } (\sigma_1)$, the control law is expressed by the following equation:

$$\alpha_1 = \frac{-\lambda_1 \text{ sign } (\sigma_1) - \gamma_1 e_1 - E}{K}. \quad (11)$$

4. Output Current Controller

Because most of the utilities are alternative, the reason to convert DC energy to AC energy becomes an important task. To perform the standalone PV system in AC energy, a DC-AC converter is the key solution. Moreover, being the reason behind transferring the maximum energy from the DC bus to the load, the sliding mode approach is used.

The modeling of the output current controller begins with the design of the sliding surface. Generally, the sliding surface is defined by the differences between the state variable and its reference [31]. In addition, being the reason to feed the AC load by an alternative sinusoidal current, the proposed strategy in Figure 6 allows us to calculate the peak current I_{ref} using a PI loop between the DC bus voltage v_{DC} and its calculated reference value v_{DCref}. Furthermore, to form a sinusoidal reference current i_{ref}, the peak current I_{ref} is multiplied to a generated sin (ωt); it should be mentioned that the AD9833 analog circuit may be used to generate the sin (ωt) once we start the

hardware implementation. The use of this circuit is due to its very low-frequency sensibility [32]. This current is used to construct the sliding surface given by

$$\sigma_2 = i_o - I_{ref} \sin(wt). \quad (12)$$

To make the switching surface stable and attractive, the Lyapunov function given by $(V_2 = (1/2)\sigma_2)$ is used and the substituting of the dynamic function $\dot{\sigma}_2 = -\lambda_2 \text{ sign}(\sigma_2)$ in the derivative of the Lyapunov function gives the law of control as follows:

$$\alpha_2 = \frac{1}{2}\left[1 + \frac{-L_0\lambda_2 \text{ sign}(\sigma_2) + (R_o + R_c) + L_o(\partial i_{ref}/\partial t)}{v_{DC}}\right], \quad (13)$$

where $\partial i_{ref}/\partial t = I_{ref} w \cos(wt)$.

According to the stability condition of the Lyapunov function which is $\dot{V}_2 = -\lambda_2|\sigma_2|$, the coefficient λ_2 must be strictly superior to zero.

5. Simulation Results

This section is divided into two parts; the first concerns the performance evaluation of the proposed controllers. For this reason, both the SM-MPPT and the output current controller have been implemented in MATLAB Simulink and tested under severe variations of atmospheric conditions. Thereafter, the second subsection presents a daily analysis of the net produced energy using the SM-MPPT and the modified incremental conductance proposed by Motahhir et al. [33], under the fluctuation of two whether profiles (sunny and cloudy).

5.1. Performance Validation. Before beginning the test performance, the used PV panel must be modeled. For this reason, the monocrystalline SM55 PV module with the datasheet parameters displayed in Table 1 has been modeled using an accurate method from the literature [26]. Thereafter, the extracted parameters using the method of Chaibi et al. and the simulation parameters are presented in Table 2.

In order to evaluate the proposed sliding model controllers, the system must be tested under a severe variation of atmospheric conditions. Hence, Figure 7 displays the used fluctuations of irradiance and temperature. Consequently, Figure 8 gives the response of the SM-MPPT. As noticed in these curves, the duty cycle in Figure 8(a) changes instantly to its optimal value with each climate variation. Furthermore, in Figure 8(b), the sliding surface converges immediately its reference state regardless of the sudden variation in irradiance. Otherwise, when the temperature varies suddenly from 25°C to 50°C, the sliding surface spikes and comebacks rapidly to the equilibrium state. To show the effect of these spikes on the output PV power, Figure 9 presents the response of the PV power for each change of irradiance and temperature. As observed, the

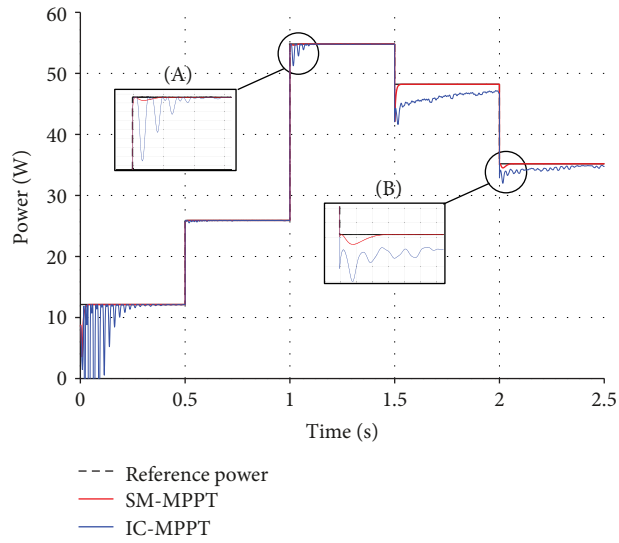

Figure 9: Output power of the SM55 PV panel using the SM-MPPT and IC-MPPT.

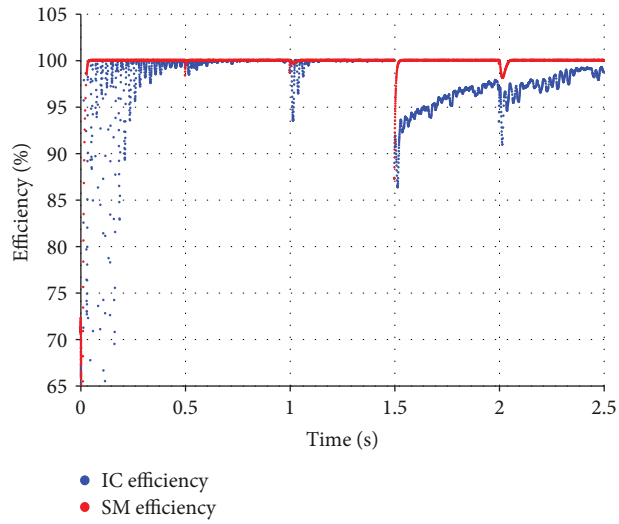

Figure 10: Tracking efficiencies of the SM-MPPT and the incremental conductance technique.

power reaches instantly the reference despite any rapid change of irradiance. For the temperature, the high increase of temperature from 25°C to 50°C causes a negligible time of response to achieve the optimal value. In addition, Figure 9 compares the controlled power with the corresponding one to the incremental conductance method and to the theoretical power. As noticed in this comparison (Figures 9(a) and 9(b)), the SM-MPPT reaches rapidly the theoretical values but the IC method takes time to attain the theoretical value. Moreover, the IC-MPPT oscillates around the optimal value and loses the tracking because of the rapid increase of temperature (see Figure 9(b)). Therefore, it can be deduced that the SM-MPPT presents high performances in terms of stability and fast response even with severe atmospheric changes.

Table 3: Performance comparison between the SM-MPPT and the IC-MPPT.

	Efficiency	Oscillations		Response time	
		Sudden change of λ	Sudden change of T	Sudden change of λ	Sudden change of T
SM-MPPT	99.10%	Neglected	Neglected	Very fast	Fast
IC-MPPT	92.16%	High	High	Slow	Very slow

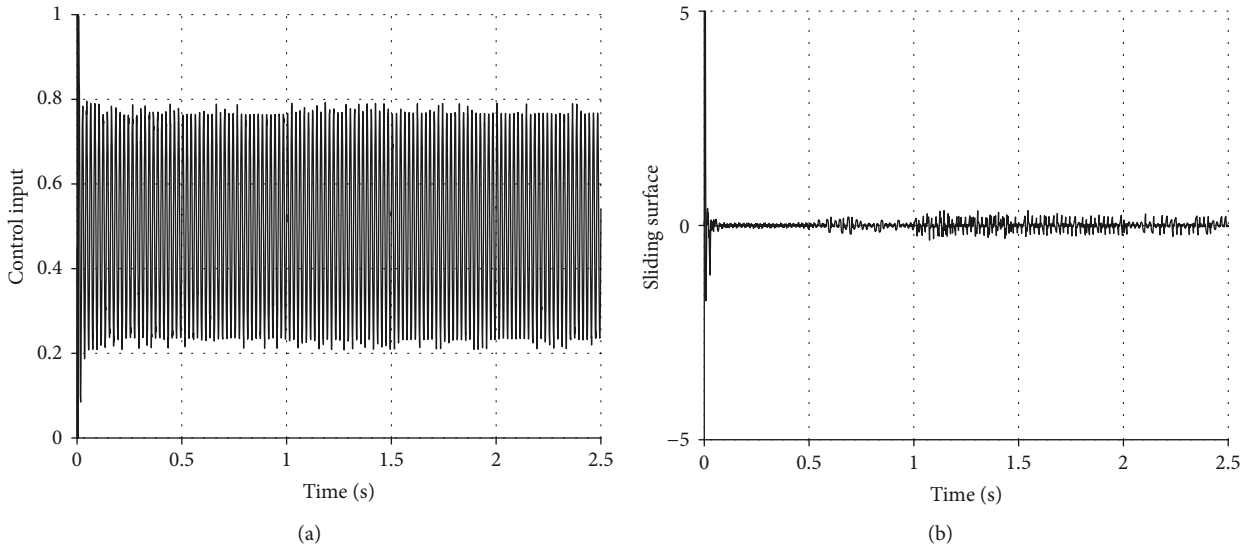

Figure 11: Control input and the sliding surface used to design the control law of the inverter.

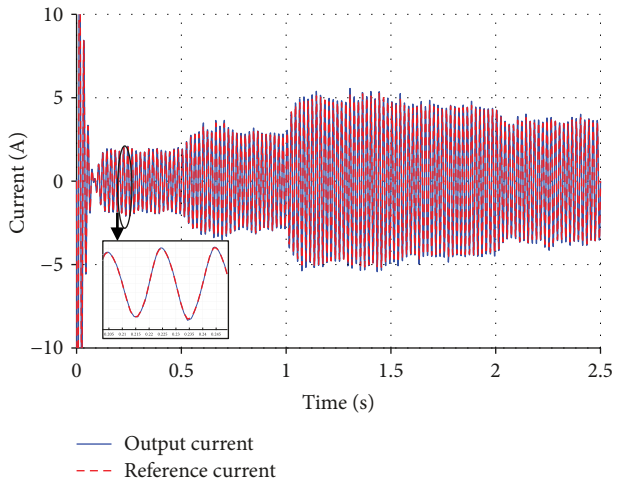

Figure 12: Reference and the controlled output current.

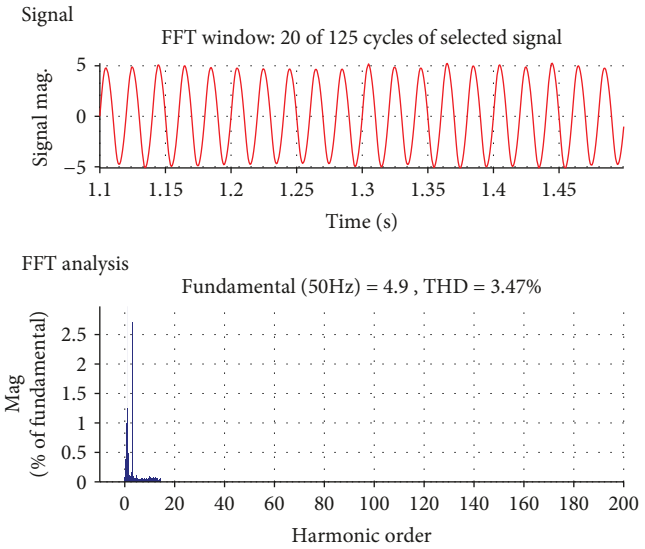

Figure 13: Harmonic distortion analysis of the controlled output current.

Besides, to make the power results accurate, the MPPT efficiency is computed using the following equation:

$$\zeta_{\text{MPPT}} = \frac{P_{\text{measured}}}{P_{\text{theoritical}}}^{*} 100, \tag{14}$$

where P_{measured} is the calculated power using the SM-MPPT or the IC-MPPT. Accordingly, these calculated efficiencies are plotted in Figure 10 for each change of irradiance and temperature. As seen in this figure, the SM-MPPT efficiency values are close to 99% for all the variations of irradiance and temperature. However, the IC efficiency changes dramatically with atmospheric variation, especially for the temperature one. These performances are summarized in Table 3 to show the comparison between the SM-MPPT and the IC-MPPT in terms of the mean tracking efficiency, the oscillation level, and the time of response. As shown, the SM-MPPT presents high performances and exceeds the IC-MPPT for any sudden change of irradiance and temperature.

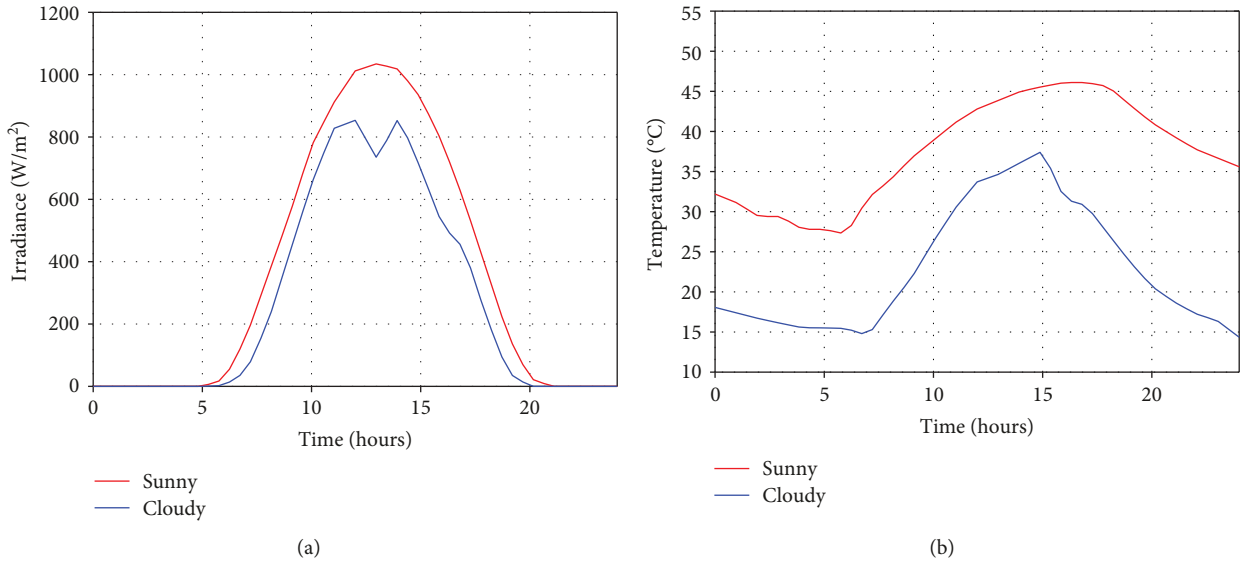

Figure 14: Daily climate condition of a sunny (a) day and a cloudy (b) day.

The second part of this subsection consists in evaluating the performance of the sliding mode output current controller. The objective of this later is to force the output current i_o to pursue the reference value of the current generated from the PI regulator. To verify this purpose, the developed input control and the sliding surface are plotted in Figure 11. As shown, the control input performs as a sinusoidal waveform with a significant fluctuation of the amplitude due to the reference current variation. Furthermore, the sliding surface oscillates around zero which means that the state variable converges to its reference value. Therefore, the controlled output current is plotted with its reference value in Figure 12. As can be seen in this curve, the output current fits perfectly with the reference current and changes its value according to the change of this reference current. The quality of this controlled current is examined using the FTT analysis. The obtained results in Figure 13 indicate that the harmonic distortion has a value of 3.47% which is less than the international standard (5%).

The previous results demonstrate the robustness and the high performance of the sliding mode controllers. In order to make these results accurate, the proposed PV system and controllers must be evaluated under real climatic fluctuations.

5.2. Daily Performance. In order to estimate the performance of the sliding mode MPPT controller, the latter and the incremental conductance technique are evaluated under a daily change of irradiance and temperature. The daily atmospheric conditions of a sunny day and a cloudy day are illustrated in Figure 14. As can be seen in Figure 14(a), the irradiance variation of both the sunny and the cloudy days is characterized by its gradual increase until the maximum values of 1035.42 W/m^2 and 863.59 W/m^2, respectively; then, a decrease till approximately the initial values can be noticed. In the case of the temperature variation (see Figure 14(b)), the sunny day presents high fluctuations between a maximum value of 46.10°C and a minimum value of 27.80°C. However, the cloudy day is characterized by its low-temperature changes compared to the sunny day profile with a variation between maximum and minimum values of 37.57°C and 14.35°C, respectively. Considering the profiles illustrated in Figure 14, the daily generated power using both whether profiles (sunny and cloudy) is displayed in Figure 15. As observed in Figure 15(a), the generated power using the climate series data of the sunny profile is presented for the SM-MPPT and the IC-MPPT. As observed in this figure, it is clear that, as expected, the SM-MPPT shows superiority for low atmospheric variations. However, at high climate levels, the corresponding powers to the IC-MPPT are close to the SM-MPPT ones. Thus, The IC technique presents good performances for high atmospheric variations but the SM-MPPT is still more accurate. Consequently, the SM-MPPT and the IC-MPPT controllers generate 423.49 Wh and 374.69 Wh of energy, respectively, which explains the superiority of the SM-MPPT. Furthermore, the SM-MPPT controller generates a surplus estimated to 13.02% of energy more than the IC-MPPT. In the cloudy climate conditions, Figure 15(b) shows accurate higher performance of the SM-MPPT compared to the incremental conductance technique; this superiority is demonstrated by the fact that the SM-based MPPT generates 332.48 Wh which significantly exceeds energy generation by the IC-MPPT (estimated at 260.63 Wh). Accordingly, the proposed SM-MPPT induces up to 27.57% of energy more than the IC-MPPT.

6. Conclusion

In this paper, robust controllers based on sliding mode theory are applied on two converters for a single-phase standalone PV system. The suggested controllers consist of SM-MPPT and an output current controller. Besides, the generation of the reference current is performed directly

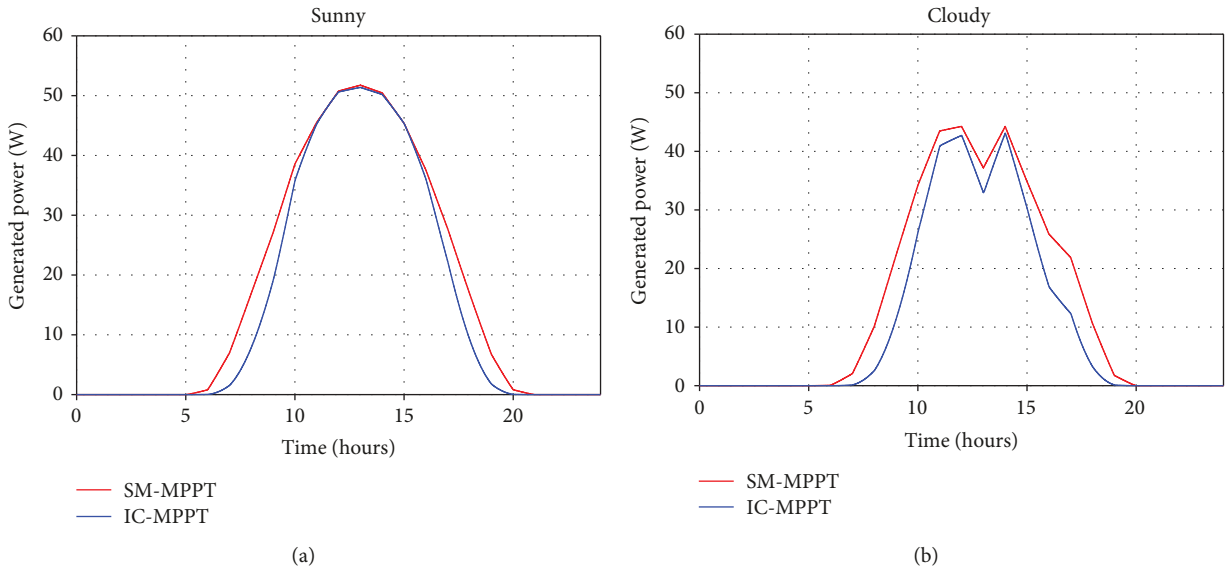

Figure 15: Daily generated power using the SM-MPPT and the IC method for sunny and cloudy whether profiles.

from the PI controller. In the presence of any sudden change of irradiance and temperature, the controllers react rapidly in order to reach the reference values without oscillation around the MPP; this proves that our method, the sliding mode with a constant reference, is better than the classical one which is based on variable steps. In addition, the system stays stable because of the Lyapunov function.

The performance of the controllers is verified through numerical simulations; the PV system results show very good tracking performances and high stability compared to the IC-MPPT. In addition, the output current has a sinusoidal form with a THD of 3.47%. Moreover, the daily performance shows that the SM-MPPT yields the highest energy compared to the IC techniques. More specifically, the suggested SM-MPPT could achieve up to 13.02% of energy for the sunny whether profile and up to 27.57% of energy for the cloudy one. Due to its high performances, the suggested controllers could be a key solution for different uses of the standalone PV system such as in isolated sites and pumping PV systems.

Appendix

Derivations of the PV current equation

$$\frac{\partial I_{pv}}{\partial V_{pv}} = \frac{-AI_{os}\exp\left[A\left(V_{pc}+R_sI_{pv}\right)\right]-\left(1/R_{sh}\right)}{1+\left(R_s/R_{sh}\right)+R_sAI_{os}\exp\left[A\left(V_{pc}+R_sI_{pv}\right)\right]}. \quad (A.1)$$

We suppose that $H = 1 + (R_s/R_{sh}) + R_sAI_{os}\exp[A(V_{pc} + R_sI_{pv})]$.

$$\frac{\partial^2 I_{pv}}{\partial V_{pv}^2} = \frac{-A^2 I_{os}\exp\left[A\left(V_{pc}+R_sI_{pv}\right)\right]\left(R_s\left(\partial I_{pv}/\partial V_{pv}\right)+1\right)}{H^2},$$

$$\frac{\partial^3 I_{pv}}{\partial V_{pv}^3} = \frac{A^3 I_{os}\exp\left[A\left(V_{pc}+R_sI_{pv}\right)\right]\left(R_s\left(\partial I_{pv}/\partial V_{pv}\right)+1\right)^2-\left(\partial^2 I_{pv}/\partial V_{pv}^2\right)\left\{R_sA^2I_{os}\exp\left[A\left(V_{pc}+R_sI_{pv}\right)\right]+2A^3I_{os}^2R_s^2\exp^2\left[A\left(V_{pc}+R_sI_{pv}\right)\right]\left(R_s\left(\partial I_{pv}/\partial V_{pv}\right)+1\right)\right\}}{H^2},$$

$$\frac{\partial P_{pv}}{\partial V_{pv}} = I_{pv} + V_{pv}\frac{\partial I_{pv}}{\partial V_{pv}},$$

$$\frac{\partial^2 P_{pv}}{\partial V_{pv}^2} = 2\frac{\partial I_{pv}}{\partial V_{pv}} + V_{pv}\frac{\partial^2 I_{pv}}{\partial V_{pv}^2},$$

$$\frac{\partial^3 P_{pv}}{\partial V_{pv}^3} = 3\frac{\partial^2 I_{pv}}{\partial V_{pv}^2} + V_{pv}\frac{\partial^3 I_{pv}}{\partial V_{pv}^3}, \quad (A.2)$$

$$\dot{y}_1 = \frac{\partial y_1}{\partial t} = \frac{\partial^2 P_{pv}}{\partial V_{pv}^2}\frac{\partial V_{pv}}{\partial t}, \quad (A.3)$$

$$\ddot{y}_1 = \left(\frac{\partial^3 P_{pv}}{\partial V_{pv}^3}\right)\left(\frac{\partial V_{pv}}{\partial t}\right)^2 + \left(\frac{\partial^2 P_{pv}}{\partial V_{pv}^2}\right)\left[\frac{1}{C}\frac{\partial I_{pv}}{\partial V_{pv}}\frac{\partial V_{pv}}{\partial t} - \frac{1}{LC}\left(v_{pv}-v_{DC}\right)\right] - \alpha_1\frac{V_{DC}}{LC}\frac{\partial^2 P_{pv}}{\partial V_{pv}^2}. \quad (A.4)$$

Equation (A.4) can be rewritten as $E + \alpha_1 K$, where

$$E = \left(\frac{\partial^3 P_{pv}}{\partial V_{pv}^3}\right)\left(\frac{\partial V_{pv}}{\partial t}\right)^2 + \left(\frac{\partial^2 P_{pv}}{\partial V_{pv}^2}\right)\left[\frac{1}{C}\frac{\partial I_{pv}}{\partial V_{pv}}\frac{\partial V_{pv}}{\partial t} - \frac{1}{LC}\left(v_{pv} - v_{DC}\right)\right],$$
$$K = \frac{V_{DC}}{LC}\frac{\partial^2 P_{pv}}{\partial V_{pv}^2}. \quad (A.5)$$

Nomenclature

C, C_{DC}: Input and output capacitor of the boost converter (F)
E_{Go}: Band gap
I_{pv}: Output current of the PV module (A)
I_{ph}: Light-generated current (A)
I_D: Current of the diode (A)
I_{Rsh}: Current following in shunt resistance (A)
I_{os}: Cell saturation current (A)
I_{or}: Reverse current of the cell (A)
I_{sc}: Short-circuit current (A)
i_L: Input current of the boost converter (A)
i_o: Output current of the inverter (A)
I_{ref}: Reference current (A)
I_{cell}: Maximum power current (A)
k: Boltzmann constant ($1.381 \cdot 10^{-23}$ J/K)
K_i: Temperature coefficient of I_{sc} (A/K)
L: Input inductance of the boost converter (H)
L_o: Inductance of the output filter (H)
N_{cell}: Number of cells in series
P_{cell}: Maximum power of the PV module (W)
q: Electron charge ($1.602 \cdot 10^{-19}$ C)
R_o: Resistance of the output filter (Ω)
R_c: Load resistance (Ω)
T, T_{ref}: Cell and reference temperatures (K)
V_{cell}: Maximum voltage of the PV module (V)
V_{oc}: Open-circuit voltage (V)
V_{DC}: Output voltage of the boost converter (V)
V_{pv}: Output voltage of the PV module (V)
γ: Ideality factor
ω: The pulsation (rad/s)
λ, λ_{ref}: Solar and reference irradiances (W/m^2).

Data Availability

The data used to support the findings of this study have not been made available because it is confidential.

Conflicts of Interest

The authors declare that they have no conflicts of interest.

References

[1] D. Elliott, "Renewable energy and sustainable futures," *Futures*, vol. 32, no. 3-4, pp. 261–274, 2000.

[2] I. Yahyaoui, M. Chaabene, and F. Tadeo, "Evaluation of maximum power point tracking algorithm for off-grid photovoltaic pumping," *Sustainable Cities and Society*, vol. 25, pp. 65–73, 2016.

[3] A. Evans, V. Strezov, and T. J. Evans, "Assessment of sustainability indicators for renewable energy technologies," *Renewable and Sustainable Energy Reviews*, vol. 13, no. 5, pp. 1082–1088, 2009.

[4] T. Kousksou, A. Allouhi, M. Belattar et al., "Renewable energy potential and national policy directions for sustainable development in Morocco," *Renewable and Sustainable Energy Reviews*, vol. 47, pp. 46–57, 2015.

[5] S. Drid, L. Chrifi-Alaoui, P. Bussy, and M. Ouriagli, "Robust control of the photovoltaic system with improved maximum power point tracking," in *2014 Ninth International Conference on Ecological Vehicles and Renewable Energies (EVER)*, pp. 1–7, Monte-Carlo, Monaco, March 2014.

[6] J. Hahm, J. Baek, H. Kang, H. Lee, and M. Park, "Matlab-based modeling and simulations to study the performance of different MPPT techniques used for photovoltaic systems under partially shaded conditions," *International Journal of Photoenergy*, vol. 2015, Article ID 979267, 10 pages, 2015.

[7] D. Verma, S. Nema, A. M. Shandilya, and S. K. Dash, "Maximum power point tracking (MPPT) techniques: recapitulation in solar photovoltaic systems," *Renewable and Sustainable Energy Reviews*, vol. 54, pp. 1018–1034, 2016.

[8] N. Femia, D. Granozio, G. Petrone, G. Spagnuolo, and M. Vitelli, "Predictive & adaptive MPPT perturb and observe method," *IEEE Transactions on Aerospace and Electronic Systems*, vol. 43, no. 3, pp. 934–950, 2007.

[9] J. Ahmed and Z. Salam, "An improved perturb and observe (P&O) maximum power point tracking (MPPT) algorithm for higher efficiency," *Applied Energy*, vol. 150, pp. 97–108, 2015.

[10] E. M. Ahmed and M. Shoyama, "Stability study of variable step size incremental conductance/impedance MPPT for PV systems," in *8th International Conference on Power Electronics - ECCE Asia*, pp. 386–392, Jeju, South Korea, May--June 2011.

[11] S. Motahhir, A. el Ghzizal, S. Sebti, and A. Derouich, "Modeling of photovoltaic system with modified incremental conductance algorithm for fast changes of irradiance," *International Journal of Photoenergy*, vol. 2018, Article ID 3286479, 13 pages, 2018.

[12] C. Ben Salah and M. Ouali, "Comparison of fuzzy logic and neural network in maximum power point tracker for PV systems," *Electric Power Systems Research*, vol. 81, no. 1, pp. 43–50, 2011.

[13] N. A. Gounden, S. A. Peter, H. Nallandula, and S. Krithiga, "Fuzzy logic controller with MPPT using line-commutated inverter for three-phase grid-connected photovoltaic systems," *Renewable Energy*, vol. 34, no. 3, pp. 909–915, 2009.

[14] A. A. Kulaksiz and R. Akkaya, "A genetic algorithm optimized ANN-based MPPT algorithm for a stand-alone PV system with induction motor drive," *Solar Energy*, vol. 86, no. 9, pp. 2366–2375, 2012.

[15] M. A. A. Mohd Zainuri, M. A. Mohd Radzi, A. C. Soh, and N. A. Rahim, "Adaptive P&O-fuzzy control MPPT for PV boost dc-dc converter," in *2012 IEEE International Conference on Power and Energy (PECon)*, pp. 524–529, Kota Kinabalu, Malaysia, December 2012.

[16] Y. Levron and D. Shmilovitz, "Maximum power point tracking employing sliding mode control," *IEEE Transactions on*

Circuits and Systems I: Regular Papers, vol. 60, no. 3, pp. 724–732, 2013.

[17] M. Farhat, O. Barambones, and L. Sbita, "A new maximum power point method based on a sliding mode approach for solar energy harvesting," *Applied Energy*, vol. 185, pp. 1185–1198, 2017.

[18] M. Sarvi, I. Soltani, N. NamazyPour, and N. Rabbani, "A new sliding mode controller for DC/DC converters in photovoltaic systems," *Journal of Energy*, vol. 2013, Article ID 871025, 7 pages, 2013.

[19] H. T. Yau, C. J. Lin, and C. H. Wu, "Sliding mode extremum seeking control scheme based on PSO for maximum power point tracking in photovoltaic systems," *International Journal of Photoenergy*, vol. 2013, Article ID 527948, 10 pages, 2013.

[20] D. Gonzalez Montoya, C. A. Ramos Paja, and R. Giral, "Maximum power point tracking of photovoltaic systems based on the sliding mode control of the module admittance," *Electric Power Systems Research*, vol. 136, pp. 125–134, 2016.

[21] L. Martinez-Salamero, A. Cid-Pastor, R. Giral, J. Calvente, and V. Utkin, "Why is sliding mode control methodology needed for power converters?," in *Proceedings of 14th International Power Electronics and Motion Control Conference EPE-PEMC 2010*, pp. 25–31, Ohrid, Macedonia, September 2010.

[22] I. S. Kim, M. B. Kim, and M. J. Youn, "New maximum power point tracker using sliding-mode observer for estimation of solar array current in the grid-connected photovoltaic system," *IEEE Transactions on Industrial Electronics*, vol. 53, no. 4, pp. 1027–1035, 2006.

[23] I.-S. Kim, "Robust maximum power point tracker using sliding mode controller for the three-phase grid-connected photovoltaic system," *Solar Energy*, vol. 81, no. 3, pp. 405–414, 2007.

[24] S. Dhar and P. K. Dash, "A finite time fast terminal sliding mode I–V control of grid-connected PV Array," *Journal of Control, Automation and Electrical Systems*, vol. 26, no. 3, pp. 314–335, 2015.

[25] A. M. Humada, M. Hojabri, S. Mekhilef, and H. M. Hamada, "Solar cell parameters extraction based on single and double-diode models: a review," *Renewable and Sustainable Energy Reviews*, vol. 56, pp. 494–509, 2016.

[26] Y. Chaibi, M. Salhi, A. El-jouni, and A. Essadki, "A new method to extract the equivalent circuit parameters of a photovoltaic panel," *Solar Energy*, vol. 163, pp. 376–386, 2018.

[27] W. Shockley and H. J. Queisser, "Detailed balance limit of efficiency of *p-n* junction solar cells," *Journal of Applied Physics*, vol. 32, no. 3, pp. 510–519, 1961.

[28] M. Taherkhorsandi, K. K. Castillo-Villar, M. J. Mahmoodabadi, F. Janaghaei, and S. M. M. Yazdi, "Optimal sliding and decoupled sliding mode tracking control by multi-objective particle swarm optimization and genetic algorithms," in *Advances and Applications in Sliding Mode Control systems. Studies in Computational Intelligence, vol 576*, A. Azar and Q. Zhu, Eds., pp. 43–78, Springer, Cham, 2015.

[29] K. Dahech, M. Allouche, T. Damak, and F. Tadeo, "Backstepping sliding mode control for maximum power point tracking of a photovoltaic system," *Electric Power Systems Research*, vol. 143, pp. 182–188, 2017.

[30] Y. Shtessel, C. Edwards, L. Fridman, and A. Levant, "Sliding mode control and observation," in *Control Engineering*, Springer, 2014.

[31] C.-S. Chiu, Y.-L. Ouyang, and C.-Y. Ku, "Terminal sliding mode control for maximum power point tracking of photovoltaic power generation systems," *Solar Energy*, vol. 86, no. 10, pp. 2986–2995, 2012.

[32] "Programmable waveform generator AD9833," http://www.alldatasheet.com/datasheet-pdf/pdf/549388/AD/AD9833.html.

[33] S. Motahhir, A. el Ghzizal, S. Sebti, and A. Derouich, "MIL and SIL and PIL tests for MPPT algorithm," *Cogent Engineering*, vol. 4, no. 1, pp. 1–18, 2017.